Altered Expression of the Early Mitotic Checkpoint Protein, CHFR, in Breast Cancers: Implications for Tumor Suppression

Lisa M. Privette,[1] Maria E. González,[2] Lei Ding,[3] Celina G. Kleer,[3] and Elizabeth M. Petty[1,2]

Departments of [1]Human Genetics, [2]Internal Medicine, and [3]Pathology, University of Michigan, Ann Arbor, Michigan

Abstract

Checkpoint with FHA and Ring Finger (CHFR) is hypothesized to mediate a delay in cell cycle progression early in mitosis in response to microtubule stress, independent of the spindle assembly checkpoint. As a potential regulator of cell cycle progression, CHFR naturally becomes an interesting target for understanding cancer cells. In recent years, there has been increasing evidence supporting the role of CHFR as a tumor suppressor, most of which report loss of expression, occasionally due to promoter hypermethylation, in cancers compared with patient-matched normal tissues. We studied both a panel of breast cancer cell lines as well as primary tissue samples from breast cancer patients to investigate CHFR as a relevant tumor suppressor in breast cancer and to determine whether CHFR expression was associated with clinical and pathologic variables. We report that 41% of cell lines and 36% of patient samples showed low or negative CHFR protein expression or staining. In addition, lack of CHFR detection was associated with increased tumor size and weakly correlated with estrogen receptor–negative tumors from patients. To study the effects of low CHFR expression *in vitro*, we stably expressed a short hairpin RNA construct targeting *CHFR* in two lines of immortalized human mammary epithelial cells. Notably, decreased CHFR expression resulted in the acquisition of many phenotypes associated with malignant progression, including accelerated growth rates, higher mitotic index, enhanced invasiveness, increased motility, greater aneuploidy, and amplified colony formation in soft agar, further supporting the role of CHFR as a tumor suppressor in breast cancer. [Cancer Res 2007;67(13):6064–74]

Introduction

Breast cancer, the second leading cause of cancer-related death among women in the United States, is often associated with defects in cell cycle checkpoint regulation. Checkpoint with FHA and Ring Finger (CHFR) is a checkpoint protein that reportedly initiates a cell cycle delay in response to microtubule stress during prophase in mitosis (1). This delay is thought to occur before chromosome condensation by excluding cyclin B1 from the nucleus (2). One form of microtubule stress is treatment with taxanes, such as nocodazole or paclitaxel (Taxol), a chemotherapeutic drug used for cancer patients, including those with breast cancer (3). Therefore, CHFR has been hypothesized to be a tumor suppressor with a potential role as a biomarker for chemotherapeutic response to Taxol (4, 5). Many reports have noted that cancer cells that have lost *CHFR* expression are more likely to undergo apoptosis in response to microtubule poisons, which strongly supports this hypothesis (1, 5–7). The molecular mechanism by which CHFR initiates a cell cycle arrest is debated, although evidence implicates the p38/mitogen-activated protein kinase pathway, an Aurora A interaction, and/or through regulation of PLK-1 (8–11).

There is evidence that *CHFR* may function, in part, as a tumor suppressor gene. Most notably, several groups have shown that *CHFR* mRNA expression is lost or decreased in primary tumors and cancer cell lines when compared with matched normal tissues and cells. The best characterized means of expression loss is promoter hypermethylation, which occurs in a subset of tumors and cell lines and the frequency of which seems to be dependent on the tissue of origin (4, 5, 12–20). Further support that *CHFR* may mediate tumorigenesis is that its chromosomal location, 12q24, is a site for allelic imbalance and chromosome rearrangements in several types of cancer (21–25). In addition, Yu et al. (11) published recently their description of a *Chfr* knockout mouse. The null mice were prone to developing tumors and mouse embryonic fibroblasts were aneuploid, suggesting a role for CHFR in genomic stability. However, to date, there has been little functional evidence describing *CHFR* as a tumor suppressor in a human model system.

To characterize the role of CHFR in breast cancer, we used both cultured breast cell lines and primary patient samples. We assessed the expression of CHFR protein and mRNA in a panel of breast cancer cell (BCC) lines and found that expression is low or absent in many of them when compared with immortalized human mammary epithelial cells (IHMEC). Analysis of a tissue microarray (TMA) composed of primary invasive breast cancer samples indicated that a significant number of patient samples showed negative or weak CHFR protein staining by immunohistochemistry and that CHFR staining was inversely correlated with tumor size. In view of this evidence that CHFR may be a tumor suppressor, we mimicked cellular loss of expression via stable short hairpin RNA (shRNA) and transient small interfering RNA (siRNA) targeting CHFR in two IHMEC lines. This decrease in expression led to the acquisition of many phenotypes associated with malignant progression.

Materials and Methods

Cell culture. Most cell lines were obtained from the American Type Culture Collection and grown under recommended conditions. SUM1315, SUM102, SUM190, SUM159, SUM149, SUM52, SUM185, SUM225, and SUM229 and the human papilloma virus (HPV)–immortalized series of nontumorigenic mammary cell lines were developed and provided by S.P. Ethier, Karmanos Cancer Institute, Wayne State University, Detroit, MI (now available from Asterand), and cultured according to specified conditions (26). A detailed description of relevant cell line information, including origins and hormone receptor status, has been compiled by Neve et al. (27). Please see Supplementary Table S1 for a brief description of the three cell lines predominantly used in this report.

Note: Supplementary data for this article are available at Cancer Research Online (http://cancerres.aacrjournals.org/).

Requests for reprints: Elizabeth M. Petty, Departments of Human Genetics and Internal Medicine, University of Michigan, 5220A MSRBIII, 1150 West Medical Center Drive, Ann Arbor, MI 48109-0638. E-mail: epetty@umich.edu.

doi:10.1158/0008-5472.CAN-06-4109

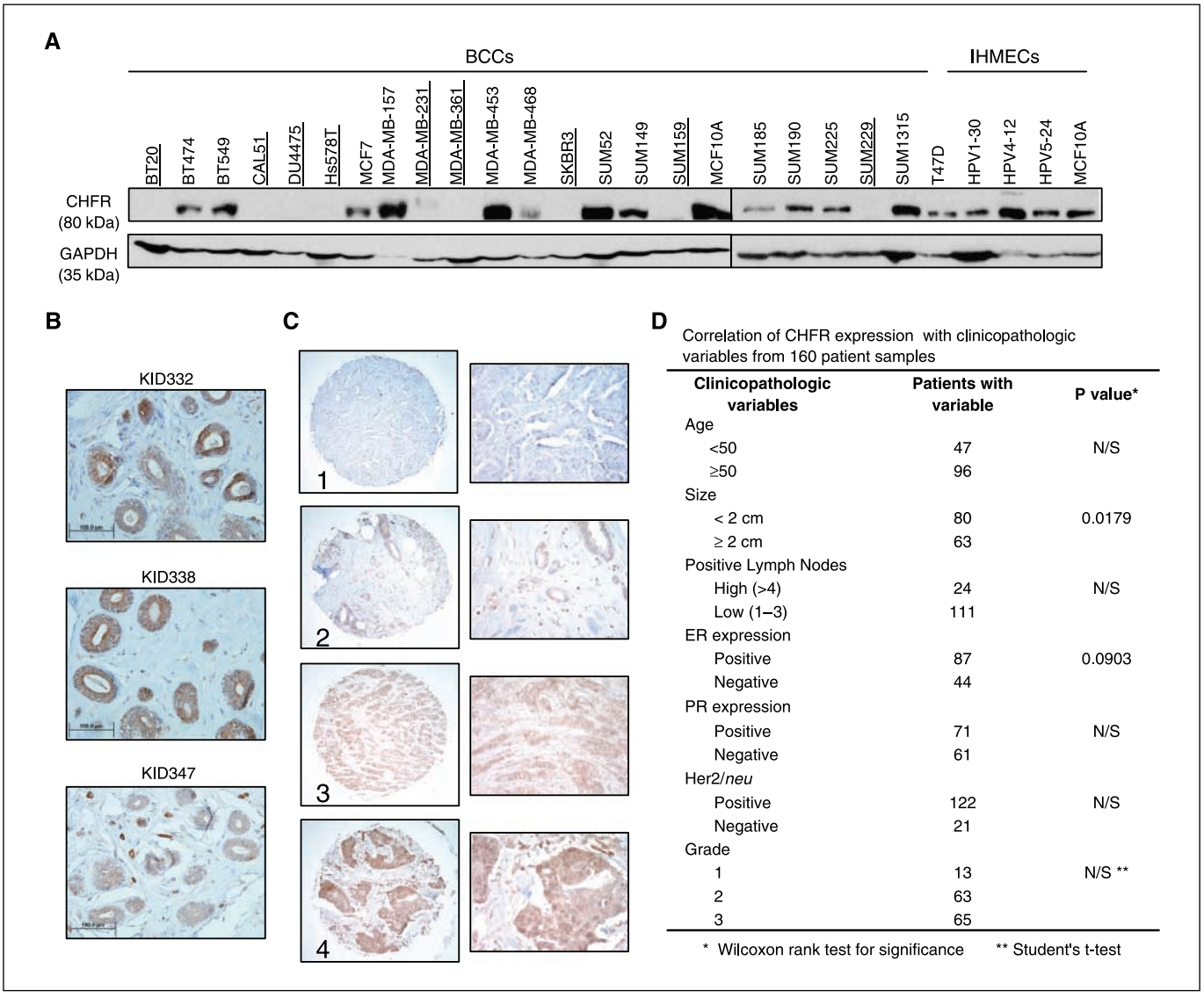

Clinicopathologic variables	Patients with variable	P value*
Age		
<50	47	N/S
≥50	96	
Size		
< 2 cm	80	0.0179
≥ 2 cm	63	
Positive Lymph Nodes		
High (>4)	24	N/S
Low (1–3)	111	
ER expression		
Positive	87	0.0903
Negative	44	
PR expression		
Positive	71	N/S
Negative	61	
Her2/*neu*		
Positive	122	N/S
Negative	21	
Grade		
1	13	N/S **
2	63	
3	65	

* Wilcoxon rank test for significance ** Student's t-test

Figure 1. CHFR protein expression is low or lost in a subset of BCCs and primary tumors when compared with "normal" IHMECs and breast tissue, and positive expression correlates with small tumor size *in vivo. A,* Western blot analysis using a monoclonal CHFR antibody reveals that 9 of 22 (41%, *underlined*) asynchronous BCC lines, or BCCs, at 70% to 80% confluence have low CHFR expression compared with the lowest level of expression observed among four asynchronous IHMECs. To control for loading, an antibody against GAPDH was used (*bottom*). A composite image of two separate Western blots. Whole-cell lysate from the MCF10A IHMEC line was used as a control on both blots in the composite image. *B,* immunohistochemistry using the monoclonal CHFR antibody showed prominent staining in the mammary gland epithelia of normal primary breast samples. Representative examples are indicated by three separate patient tissues: KID332, KID338, and KID347. *C,* immunohistochemistry using a mAb against CHFR on primary invasive breast cancers from a TMA shows a range of CHFR expression. Intensity of CHFR staining ranged from negative (*1*) to weak (*2*), moderate (*3*), and strong (*4*). Magnifications, ×10 (*left*) and ×40 (*right*) from sections of the adjacent image. *D,* statistical analyses of clinicopathologic characteristics from 142 primary invasive breast carcinoma samples indicate that positive CHFR expression correlates strongly with small (<2 cm) tumor size and has a weaker association with ER positive (ER+) status. A sample was determined to be positive for CHFR if its staining intensity scored at a 2, 3, or 4. *P* values were calculated using the Wilcoxon rank test, except for tumor grade (*) for which the *P* value was calculated using Student's *t* test.

For retroviral transduction, PT67 packaging cells were transfected using Fugene 6 with 10.0 μg pRNA-H1.1/Hygro vector (GenScript Corp.) containing either a scrambled sequence or a CHFR shRNA construct targeting nucleotides 324 to 344, 1491 to 1511, or 2497 to 2517 (accession no. AF170724). We used the pLPCX retroviral vector for overexpression of full-length *CHFR* in Hs578T cells (Clontech Laboratories). Virus was collected after 48 h and purified with a 0.45-micron filter. Equal parts of retrovirus-containing media and normal growth media were added to 1×10^6 cells. Fresh medium was added 24 h later and selection with 20.0 μg/mL hygromycin (pRNAH1.1) or 1.5 μg/mL puromycin (pLPCX) began 48 h after infection. The resulting polyclonal cell population stably expressing the *CHFR* construct(s) was subsequently used for experimentation. MCF10A cells were transduced with all three shRNA constructs, whereas HPV4-12 cells were transduced with the shRNA construct targeting nucleotides 324 to 344 to achieve maximum knockdown.

Transient transfection of siControl or a pool of four siRNAs targeting *CHFR* (si*GENOME*, Dharmacon RNA Technologies) was done according to the manufacturer's instructions. HPV4-12 cells were transfected using Dharmafect2 lipofection reagent and MCF10A cells with Dharmafect1. For both methods, stable shRNA and transient siRNA, knockdown of CHFR expression was confirmed using semiquantitative duplex reverse transcription-PCR (RT-PCR) and Western blotting followed by densitometry.

Western blotting. To assess CHFR protein levels in asynchronous cells, 60.0 μg of total protein from 70% to 80% confluent cell cultures were separated on 10% SDS-PAGE gels using the Criterion or Ready gel systems (Bio-Rad Laboratories) and immunoblotted to Hybond-P polyvinylidene

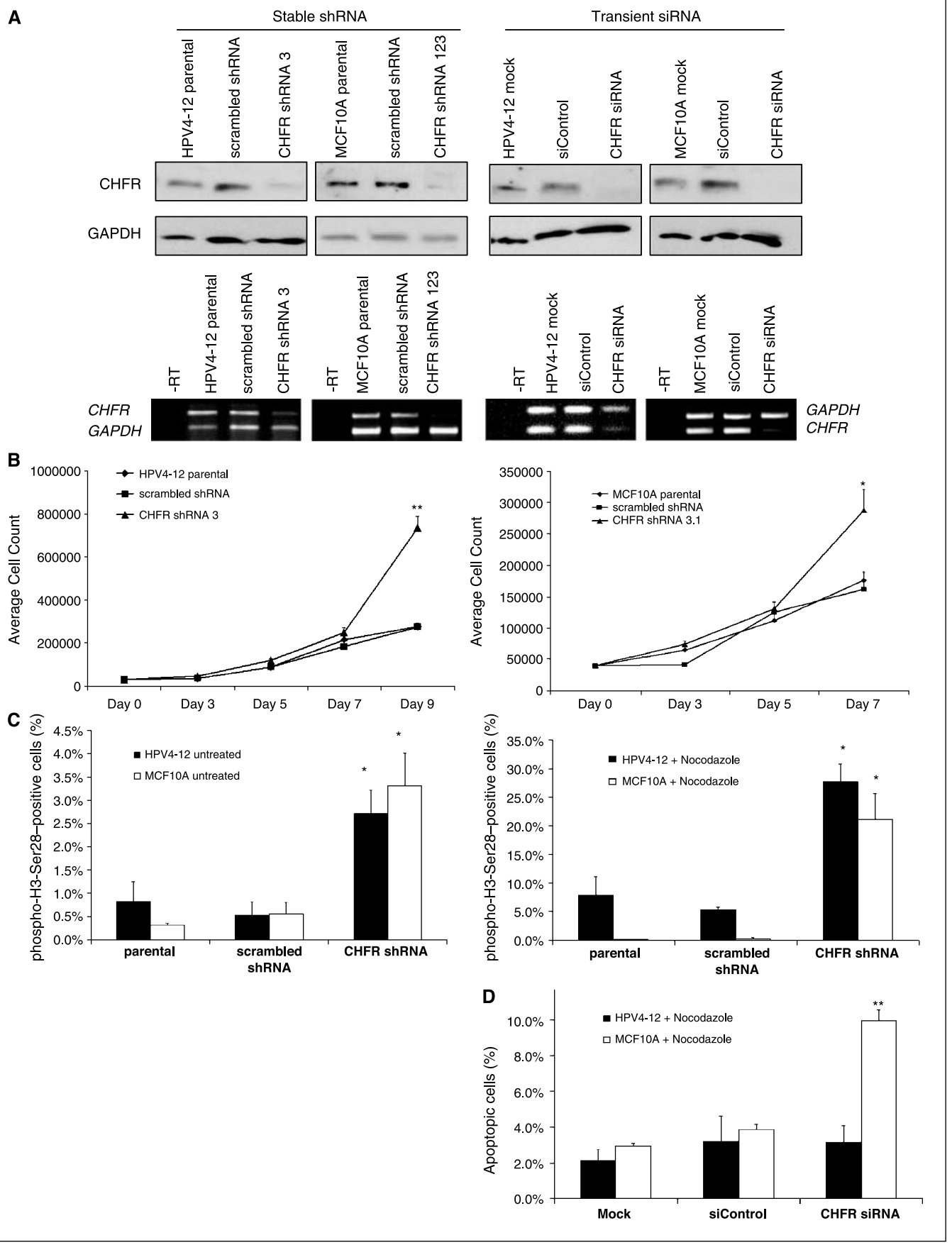

difluoride membrane (Amersham Biosciences). Following 1 h of incubation in a blocking solution of 2.5% nonfat dry milk and 0.1% TBS-Tween 20, a monoclonal antibody (mAb) against CHFR (Abnova) was used at a 1:500 dilution in 2.5% nonfat dry milk and 0.05% TBS-Tween 20 and incubated overnight at 4°C. CHFR was detected by hybridization with a goat anti-mouse/horseradish peroxidase (HRP) secondary antibody (Cell Signaling Technology) at a 1:2,000 dilution in 2.5% nonfat dry milk and 0.05% TBS-Tween 20. For a loading control, blots were blocked in 5% nonfat dry milk and 0.1% TBS-Tween 20 for 1 h. The blots were then stripped and immunoblotted again with an antibody against glyceraldehyde-3-phosphate dehydrogenase (GAPDH) as a control. The anti-GAPDH antibody (Abcam) was used at a 1:10,000 dilution and detected with a goat anti-mouse/HRP antibody at a 1:5,000 dilution, both in 5% nonfat dry milk and 0.05% TBS-Tween 20. The SuperSignal West Pico chemiluminescent kit (Pierce) was used for detection and blots were exposed to Kodak Biomax XAR film. Relative expression of CHFR was assessed by using the IS-1000 Digital Imaging System (Alpha Innotech Corp.) for densitometry to determine signal intensity, and then a ratio of CHFR/GAPDH was calculated. CHFR expression was considered low if the ratio of relative expression was <0.5, which was the lowest value among the IHMEC lines.

RT-PCR. For semiquantitative duplex RT-PCR, reaction conditions were optimized as described previously (28). Briefly, primer concentrations were optimized to create equal band intensity between *CHFR* and the internal *GAPDH* loading control, and the cycle number that resulted in the logarithmic phase of product generation was determined. Total RNA was isolated from BCCs and IHMECs via the Qiagen RNeasy RNA isolation kit. cDNA was then generated from 1.0 μg of total RNA using the Qiagen Omniscipt Reverse Transcription kit (Qiagen, Inc.) and random hexamer primers. CHFR cDNA was amplified with the following primers (forward/reverse, 5′-3′): CAGCAGTCCAGGATTACGTGTG/AGCAGTCAGGACGGGATGTTAC (500 bp) or TCCCCAGCAATAAACTGGTC/GTATGCCACGTTGTGTTCCG (205 bp). GAPDH cDNA was amplified with the following primers (forward/reverse, 5′-3′): AGTCCATGCCATCACTGCCA/GGTGTCGCTGTTGAAGTCAG (340 bp). PCR products were separated on a 1.0% agarose gel in 1× Tris-borate EDTA and stained with ethidium bromide. Band intensity was assessed using the IS-1000 Digital Imaging System.

For quantitative RT-PCR, cDNA samples from IHMECs and BCC lines were amplified in triplicate from the same total RNA sample following the manufacturer's instructions. Samples were amplified using Taqman MGB FAM dye-labeled in an ABI7900HT model Real-time PCR machine (Applied Biosystems). To amplify *CHFR* cDNA, probe set Hs00217191_m1 was used, whereas the control, *GAPDH,* was amplified with probe set Hs99999905_m1 (Applied Biosystems).

Tissue samples and immunohistochemistry. The monoclonal anti-CHFR antibody was used at a 1:50 dilution for hybridization to paraffin-embedded sections of human breast tissue using standard methods. Primary antibody was detected following protocols described by the manufacturer (DakoCytomation), using diaminobenzidine as a chromogen and with Harris hematoxylin counterstain (Surgipath Medical Industries). Optimization and validation of the immunostaining conditions was done on multi-organ TMAs using a DAKO autostainer.

To study CHFR expression in primary breast cancers, 160 paraffin-embedded patient samples arrayed on a single high-density TMA were used for the analysis (29). Details on this TMA have been described previously (30). Tissue cores from 98 patients with invasive breast carcinoma were available to evaluate CHFR staining. The staining was scored using a four tiered scoring system (1, negative; 2, weak; 3, moderate; and 4, strong) by two independent trained investigators in the Department of Pathology (C.G.K. and L.D.) and ChromaVision computerized scoring (Clarient, Inc.). The Wilcoxon rank test was used to determine if there was an association between CHFR staining and clinicopathologic variables, including patient age, tumor size, tumor grade, lymph node status, estrogen receptor (ER), progesterone receptor (PR), HER2/*neu* status, and patient survival. To determine CHFR staining in normal mammary epithelia, paraffin-embedded tissues from patients were prepared as above. Digital images were obtained with an Olympus BX-51 microscope and SPOT camera system at either a ×40 or ×60 objective magnification.

Growth curve analysis. To determine the growth rate of the cellular population, 4×10^4 cells were plated into each well in six-well plates. Cells from three different wells were then manually counted with a hemacytometer. A new set of three wells were counted every 2 to 3 days for a total of 7 or 9 days, at which point at least one cell line began to reach confluence. Average cell numbers from the three wells were then plotted as a function of a time.

Immunofluorescence and mitotic index. Early mitotic chromosomes were identified via immunofluorescence using a phospho–histone H3-Ser28 antibody (Upstate) at a 1:100 dilution and anti-rabbit Alexa Fluor 488 secondary antibody at a 1:500 dilution both diluted in blocking solution. Cells were blocked in 5% nonfat dry milk, 1% bovine serum albumin (BSA), and 0.025% Triton X-100 solution in PBS for 1 h before incubation with primary antibody. Cells were counterstained with phalloidin conjugated to Alexa Fluor 568 to detect the actin cytoskeleton and ProLong Gold antifade reagent with 4′,6-diamidino-2-phenylindole (DAPI) to detect all nuclei (both available from Molecular Probes/Invitrogen). Cells were visualized using a compound Leica DMRB microscope with a Leitz laser at ×63 magnification (W. Nuhsbaum, Inc.). The mitotic index was calculated as the number of H3-Ser28–stained nuclei from 1,000 total (DAPI stained) nuclei and then converted to a percentage.

To assess for vimentin staining, cells were plated 24 h before staining at a density of 3×10^4 cells per chamber in two-chambered slides. MCF10A cells that were transiently transfected with a pool of four *CHFR* siRNAs were transfected 48 h before seeding for immunofluorescence. Cells were blocked in 5% nonfat dry milk, 1% BSA, and 0.025% Triton X-100 solution in PBS for 1 h before incubation with primary antibody. Staining was done using an anti-vimentin antibody (1:40; Sigma-Aldrich), which was hybridized in blocking buffer overnight at 4°C, and detected with an anti-mouse/Alexa Fluor 594 secondary antibody in blocking buffer for 1 h at room temperature. Cells were counterstained with phalloidin/Alexa Fluor 488 and preserved in ProLong Gold antifade mounting media with DAPI. Cells were visualized using a compound Leica DMRB microscope with a Leitz laser at ×63 magnification and an Optronics camera system.

Apoptosis assay/Annexin V detection. Cells were seeded at 3×10^5 cells per well in six-well plates and transiently transfected with *CHFR* siRNA

Figure 2. A decrease in CHFR expression in IHMECs causes increased population growth rates, a higher number of cells entering metaphase (mitotic index), and an impaired checkpoint response to nocodazole. *A, top,* Western blotting shows a dramatic loss of CHFR protein following stable shRNA expression by retroviral transduction and transient siRNA transfection. HPV4-12 with CHFR shRNA 3 had at least a 60% decrease, whereas MCF10A with CHFR shRNA 123 showed nearly an 80% stable knockdown of CHFR expression compared with parental and scrambled shRNA controls. Transient siRNA transfection resulted in a 95% decrease in HPV4-12 cells and an ~99% decrease in MCF10A cells of CHFR protein. *Bottom,* semiquantitative duplex RT-PCR indicates a corresponding decrease in *CHFR* mRNA levels by ~70% for each cell line compared with controls. *B,* growth curves for HPV4-12 cells (*left*) and MCF10A cells (*right*) following stable shRNA expression (▲) compared with the parental cell lines (♦) and the scrambled shRNA (■) negative control cell lines. Cells were counted in triplicate every 2 days until at least one line reached confluency. *Points,* average number of cells counted on each day per cell line. Cells with decreased CHFR expression by shRNA had a faster growth rate compared with the parental and scrambled shRNA controls. *C,* the mitotic index of cells with or without CHFR shRNA is represented as the average percentage of histone H3-Ser28–stained nuclei, which is a marker of early metaphase cells, of ≥1,000 total (DAPI stained) nuclei from triplicate experiments for each cell line. Cells were either untreated (*left*) or treated with 0.67 μmol/L nocodazole (*right*) to test for checkpoint response. Cells with decreased CHFR expression by shRNA showed approximately a 6-fold increase in mitotic cells without treatment and a 4- or 10-fold increase in mitotic cells after nocodazole treatment when compared with the parental and scrambled shRNA controls. *D,* transiently decreasing CHFR by siRNA in MCF10A cells, but not HPV4-12 cells, results in an increase in apoptosis in response to nocodazole. An Annexin V antibody was used to detect the presence of Annexin V on the cell surface. Cells were counterstained with propidium iodide and assessed by flow cytometry. Percentage of Annexin V–positive and propidium iodide–negative (apoptotic) cells. *, $P \leq 0.05$; **, $P \leq 0.001$, as determined by ANOVA.

or the siControl negative control as described previously. Fifty-two hours after transfection, cells were treated with either 0.67 μmol/L nocodazole or 1.0 μmol/L paclitaxel for 20 h. Cells were then collected and labeled for Annexin V on the cell surface and DNA was stained with propidium iodide using the Vybrant Apoptosis Assay kit 2 according to the manufacturer's instructions (Molecular Probes/Invitrogen). Cells were then analyzed by flow cytometry and the apoptotic cells were those that stained for Annexin V on the cell surface but were negative for propidium iodide staining. The graphs presented indicate the percentage of apoptotic cells as assessed by flow cytometry.

Matrigel invasion assay. This invasion assay was done according to the manufacturer's instructions (BD Biosciences). In short, 2.5×10^4 cells suspended in media without chemoattractant were plated in triplicate in Matrigel baskets in a 24-well plate. In the chamber below the baskets, either media without chemoattractant as a negative control or media with chemoattractant were added. Chemoattractants for each cell line are the following: (*a*) HPV4-12 cells: 5% fetal bovine serum (FBS), 1.0 μg/mL hydrocortisone, 10.0 μg/mL insulin, 100.0 ng/mL cholera toxin, and 10.0 ng/mL epidermal growth factor (EGF); (*b*) MCF10A cells: 10% horse serum, 0.5 μg/mL hydrocortisone, 100.0 ng/mL cholera toxin, 10.0 μg/mL insulin, and 20.0 ng/mL EGF; and (*c*) Hs578T cells: 10% FBS and 10.0 μg/mL insulin.

Cells were incubated for 22 h at 37°C in 5% CO_2 for MCF10A and Hs578T cells or 10% CO_2 for HPV4-12 cells. The interior of the chambers was cleaned and the cells on the exterior were fixed and stained using the PROTOCOL Hema 3 staining kit (Fisher Scientific Co.). The number of stained cells that had traveled through the Matrigel collagen matrix was counted using a Nikon TMS inverted microscope at ×10 magnification.

Scrape motility assay. Cells were grown to confluency in six-well plates and the cell monolayer was mechanically scarred using a plastic pipette tip. Cells were visualized for movement into the scratched surface with a Leica DMIRB inverted microscope with phase-contrast optics and a 10× objective lens. Images were captured with a SPOT camera system (Diagnostic Instruments, Inc., Sterling Heights, MI). The motility phenotype was quantified by using the ImageQuant version 5.2 software package (GE Healthcare/Amersham Biosciences) to determine the area of the initial scrape and then the area of the same wound 24 h later. Data are presented as the percentage of the scraped area that remains after the end point.

Cellular morphology. Cellular morphology was recorded when cultured cells reached 100% confluence. Images were gathered using a Leica DMIL inverted microscope (W. Nuhsbaum) at ×10 magnification and a SPOT RT Color camera with SPOT Advanced digital imaging software (Diagnostic Instruments).

Soft agar assay for colony formation. To do the soft agar assay, an underlayer of a 1:1 mixture of 1.2% noble agar and cell line appropriate growth media with 40% serum was added to six-well plates and allowed to solidify at room temperature for ~15 min. To create the overlayer for each well, we combined 2.0 mL growth media with 40% serum, 1.0 mL of 1.2% noble agar, 0.6 mL water, and 1.0×10^4 cells and added it on top of the solidified underlayer. The solution solidified at room temperature for 15 min. Cells were maintained at 37°C in a humidified incubator with the appropriate levels of CO_2 and two to three drops of media were added to each well every 3 days. After 30 days, the number of colonies present in the overlayer was counted manually.

Ploidy status and nucleolar changes. Cells were collected at 70% confluence by trypsinization and resuspended in 0.075 mol/L KCl on ice for 30 min. Cells were fixed in a 3:1 mixture of methanol and glacial acetic acid with mild vortexing, dropped onto glass slides, and stained with 544 μg/mL Giemsa solution. To determine ploidy, the number of chromosomes was counted in at least 25 metaphases for each cell line and its derivatives.

To assess nucleolar changes, cells were prepared as described above and the number of nucleoli was counted in at least 50 cells, in triplicate, for each cell line. For both methods listed here, images were recorded with a compound Leitz DMRB microscope at ×40 magnification and an Optronics camera.

Statistical analysis. The ANOVA test was used to determine statistical significance when comparing quantitative phenotypic differences between parental, negative control, and CHFR-altered cells. The Wilcoxon signed-rank test and the Student's *t* test were done to assess statistical significance when analyzing patient data from the TMA. Student's *t* test was used to confirm a lack of statistical significance between parental and negative control cells for each experiment. For all tests, statistical significance was defined as $P \leq 0.05$. Error bars in the graphs presented here represent the SE.

Results

CHFR expression in BCC lines. We initially did Western blotting to assess CHFR expression in BCC and IHMEC lines. We noted variable expression among the BCC lines. Densitometry analysis revealed that 41% (9 of 22) of asynchronous BCC lines seemed to have low or no CHFR expression compared with the lowest amount of expression observed among four IHMEC cell lines, whereas only one cell line, MDA-MB-157, had expression higher than the range observed in IHMEC cells (Fig. 1*A*). The remaining lines had expression levels that fell within the range of IHMEC cells.

Previous reports indicated that *CHFR* mRNA was low in 50% of BCC lines as assessed by Northern blot analysis (31). In this study, quantitative RT-PCR was used to better define the levels of *CHFR* mRNA from asynchronous BCC lines compared with IHMECs. mRNA was collected from cells at 70% to 80% confluency, the same confluency used for Northern blot analysis. Quantitative RT-PCR revealed that only 17% of BCCs show *CHFR* expression levels significantly lower than IHMECs (data not shown). The difference between Northern blot analysis and quantitative RT-PCR may be due to the much higher sensitivity of quantitative RT-PCR to low amounts of sample or perhaps some transcripts were more easily detected by the quantitative RT-PCR probe compared with the probe used for Northern blotting. The lack of a direct correlation between mRNA levels by quantitative RT-PCR and protein expression suggests that CHFR protein expression may be altered by post-transcriptional or post-translational modification.

CHFR expression in primary breast cancers. As expected, CHFR staining by immunohistochemistry was prominent in the mammary gland epithelia from normal primary breast tissue (Fig. 1*B*). We next wanted to determine if CHFR expression was altered in primary breast cancers and if expression correlated with clinical and pathologic patient variables. From 160 patient samples of invasive breast carcinoma present on the TMA, 142 were available to score for CHFR staining and 98 had complete clinicopathologic data for statistical analysis. Of the 142 patient samples of invasive breast cancer scored for CHFR staining, 36% were negative, but only 0.5% showed strong CHFR staining. The numbers of patient samples per staining score are as follows: negative (1), 51; weak (2), 35; moderate (3), 48; and strong (4), 8 (Fig. 1*C*). Patient samples were annotated for several clinicopathologic variables, including tumor size, ER status, PR status, HER2/*neu* expression, lymph node status, patient age, and tumor grade. Primary samples were classified as positive for CHFR staining and expression if they scored between two and four in staining intensity. Because there is no published evidence as to a threshold of expression that is required for proper CHFR function, we included all positively stained samples in our analysis. Interestingly, there was a trend toward positive CHFR staining being correlated with ER-positive tumors ($P = 0.0903$, Wilcoxon rank test; $P = 0.0653$, *t* test; Fig. 1*D*). There was a striking significant correlation between positive CHFR staining and small (<2 cm) tumor size ($P = 0.0179$, Wilcoxon rank test).

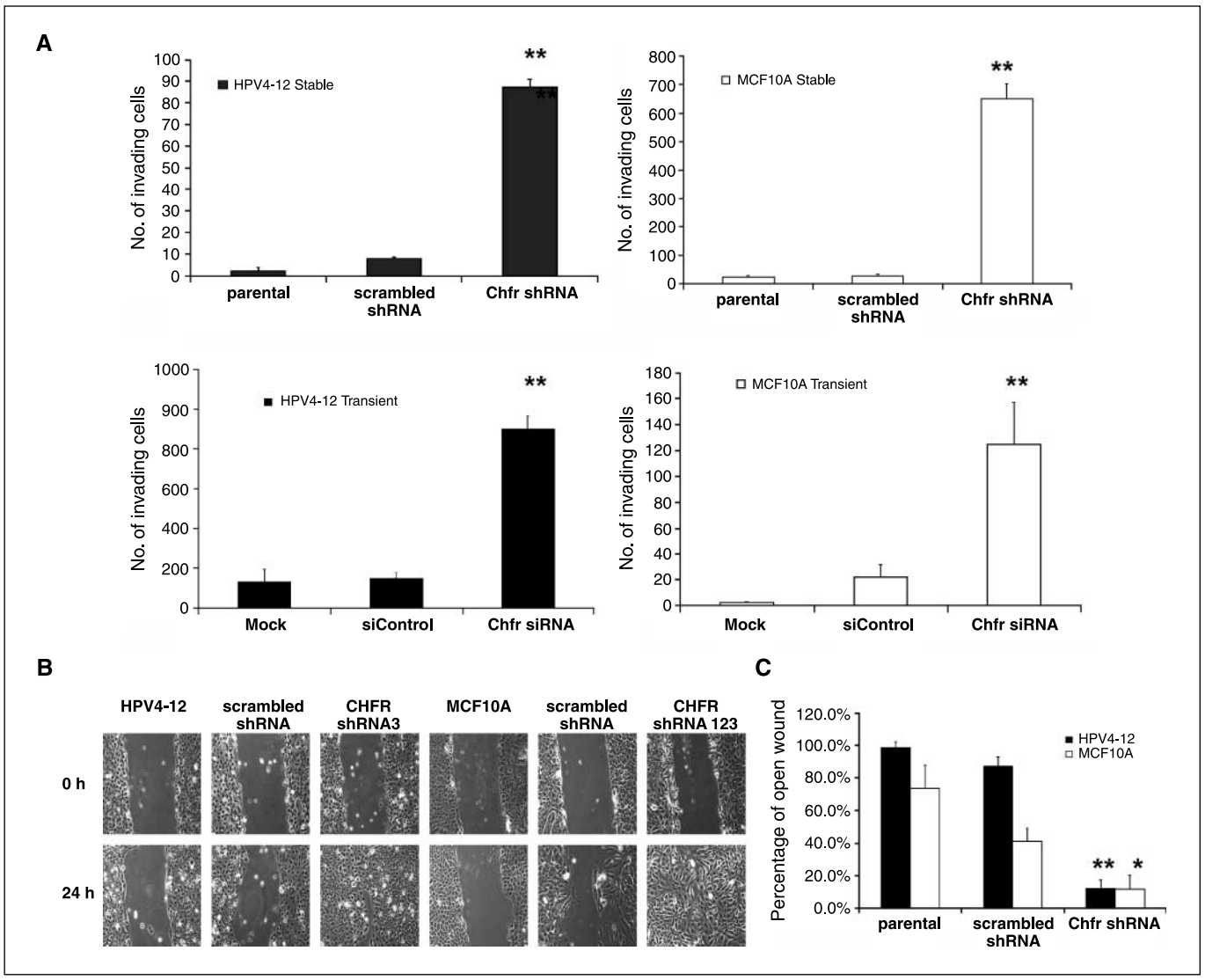

Figure 3. Decreasing CHFR expression using shRNA and siRNA in IHMECs leads to dramatic increases in invasive potential and motility. *A,* both stable (*top*) and transient (*bottom*) knockdown of CHFR expression results in greatly increased invasive potential through a Matrigel collagen matrix for both HPV4-12 cells (*left*) and MCF10A cells (*right*) compared with the control cell lines (parental/mock-transfected and scrambled shRNA/siControl). *Top left,* HPV4-12 with stable CHFR shRNA; *top right,* MCF10A with stable CHFR shRNA; *bottom left,* HPV4-12 with transient CHFR siRNA; *bottom right,* MCF10A with transient CHFR siRNA. *B,* digital phase-contrast images at ×10 magnification showing an increase in motility (closing a scraped wound in confluent culture) for HPV-12 (*far left*) and MCF10A (*middle*) cells following stable CHFR shRNA expression compared with controls. *Top,* the initial wound in the culture; *bottom,* wound closure after 24 h (MCF10A) or 48 h (HPV4-12). *C,* graphical representation of the degree of wound closure depicted above. Motility is described as the percentage of the original wounded area that remains vacant after incubation. The area of the vacant surface was calculated using ImageQuant version 5.2 software. **, $P \leq 0.001$, ANOVA testing.

Stable loss of CHFR results in increased growth rates and impairs the checkpoint. CHFR expression was significantly decreased using a stably expressed shRNA construct, as determined by Western blotting and semiquantitative duplex RT-PCR, in two IHMEC lines, HPV4-12 and MCF10A (Fig. 2*A*). Stable expression of shRNA reduced the amount of CHFR protein by at least 60% in HPV4-12 cells and by ~80% in MCF10A cells and reduced the amount of mRNA by ~70% as determined by densitometry.

We first noticed that when CHFR expression was decreased by shRNA, the population growth rate dramatically increased for both IHMECs by at least 3-fold over the course of 7 to 9 days (MCF10A, $P \leq 0.03$; HPV4-12, $P \leq 0.001$; Fig. 2*B*). To understand this increase in population growth, we assessed the percentage of mitotic cells by using immunofluorescence to stain cells for the mitotic marker phospho–histone H3-Ser28, a residue that is phosphorylated during metaphase and is gradually dephosphorylated in anaphase and is associated with the initiation of chromosome condensation (32). CHFR has been shown to delay chromosome condensation as part of the checkpoint response (2). Therefore, phospho-H3-Ser28 as a marker of condensed chromosomes is a good method to determine if the cells have passed through the CHFR checkpoint and entered the later stages of mitosis. This method was also used to determine mitotic index, which was calculated as the percentage of phospho-H3-Ser28–positive cells in the population. There was a statistically significant, 5- to 6-fold increase in the number of H3-Ser28–stained (mitotic) cells in the population when CHFR expression was lowered by shRNA in both cell lines. This showed that more cells went through the CHFR checkpoint, entering the later stages of

mitosis, with or without the stress of microtubule poisons, such as nocodazole ($P < 0.05$; Fig. 2*C*). In addition, the increase in phospho-H3-Ser28–positive cells following nocodazole treatment indicated that the checkpoint response to microtubule stress was bypassed when CHFR expression was decreased by shRNA (Fig. 2*C, right*). A similar increase in H3-Ser28 phosphorylation was observed when HPV4-12 cells were transiently transfected with a pool of four siRNAs for 72 h before staining to decrease CHFR protein by ~95% (Fig. 2*A*; data not shown).

To determine if significantly decreasing CHFR expression would alter the apoptotic response of the cells, we tested untreated or nocodazole-treated cells for the presence of Annexin V on the cell surface by flow cytometry and used propidium iodide staining to differentiate between apoptotic and necrotic cells (33). We found no difference between the cell lines with and without CHFR when they were untreated, which suggested that the increase in growth rates observed in the cells was not due to a decrease in cell death. In addition, there was no statistically significant difference in HPV4-12 cells transiently transfected with *CHFR* siRNA when compared with the mock- and siControl-transfected cells following treatment with nocodazole. However, when CHFR expression was transiently decreased in MCF10A cells, there was a 3-fold increase in apoptotic cells following nocodazole treatment ($P < 0.05$; Fig. 2*D*).

The stable loss of CHFR leads to enhanced invasive potential and increased motility. To determine if decreasing CHFR expression would cause phenotypic changes reminiscent of cellular transformation, IHMECs with or without *CHFR* shRNA were subjected to the Matrigel invasion assay and the scrape (wound) motility assay. Surprisingly, there was a dramatic increase in the ability of the cells to invade through the Matrigel collagen matrix when CHFR expression was low: a 23-fold increase for MCF10A cells and a 5-fold increase for HPV4-12 cells ($P \leq 0.001$ for both; Fig. 3*A*). This dramatic change was also observed after transient transfection with a pool of four siRNAs, each targeting a different locus in *CHFR*, which indicated that this phenotype is directly caused by CHFR loss and is not a result of clonal selection during culture of the stable shRNA lines (Fig. 2*A*; Fig 3*A, bottom*).

To assess changes in cellular motility, a wound was created in a confluent culture of IHMEC cells with or without *CHFR* shRNA. Motility was described as the percentage of the area of the initial wound that remained after a recovery period. IHMEC lines are not readily motile when their growth surface has been damaged and the remnants of the initial wound are clearly visible days later. However, when CHFR expression was decreased by stable shRNA, the cells became so motile that the wound was nearly entirely closed after 24 h (Fig. 3*B* and *C*). This was not a function of the increased population growth rates as cells with filopodia were clearly seen in the center of the wound <24 h later. In addition, the assay was completed before the population doubling time as indicated in the growth curves presented in Fig. 2*B*.

Stably decreased levels of CHFR causes morphologic changes and induces colony formation in soft agar. Normally, cells contain only one or two nucleoli in a nucleus and one frequently characterized change in cancer cells is increased number

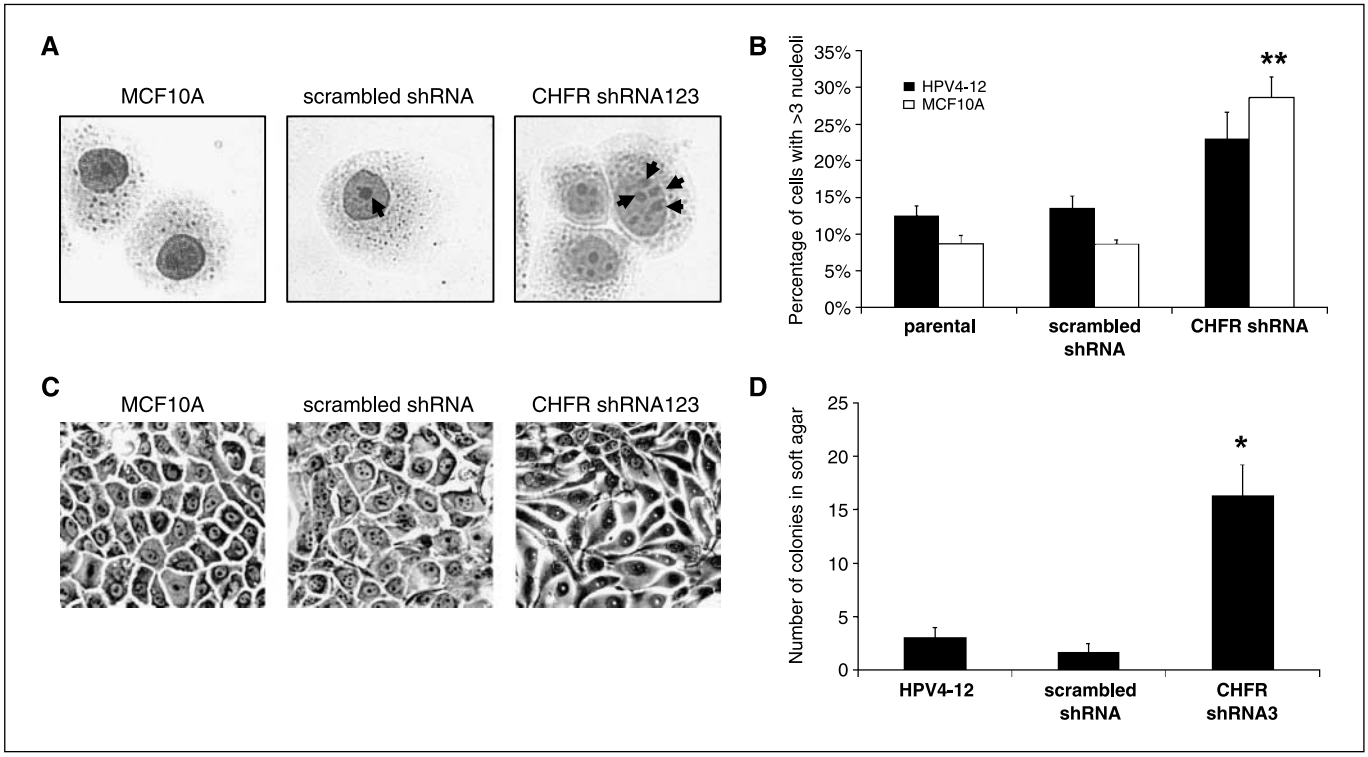

Figure 4. Decreasing CHFR expression causes nucleolar and morphologic changes and results in increased colony formation in soft agar. *A,* Giemsa-stained cells in which the nucleolus is depicted as a dark spot within the nucleus. Parental (*far left*) and scramble shRNA controls (*middle*) normally contain one or two nucleoli, whereas CHFR shRNA cells more frequently had greater than three nucleoli (*arrows*). *B,* graphical representation of the percentage of cells with greater than three nucleoli for each cell line ($n = 50$ for each of three trials). *C,* MCF10A cells visualized by phase-contrast light microscopy show a change in cellular shape from epithelial to an elongated morphology reminiscent of an epithelial-to-mesenchymal transition when CHFR expression is decreased by shRNA expression. *D,* 3-fold increase in colonies formed by HPV4-12 cells when CHFR expression is decreased. Ten thousand cells were suspended in a mixture of noble agar and complete growth media and allowed to grow for 30 d. *, $P < 0.05$; **, $P \leq 0.001$, as calculated with the ANOVA test for significance.

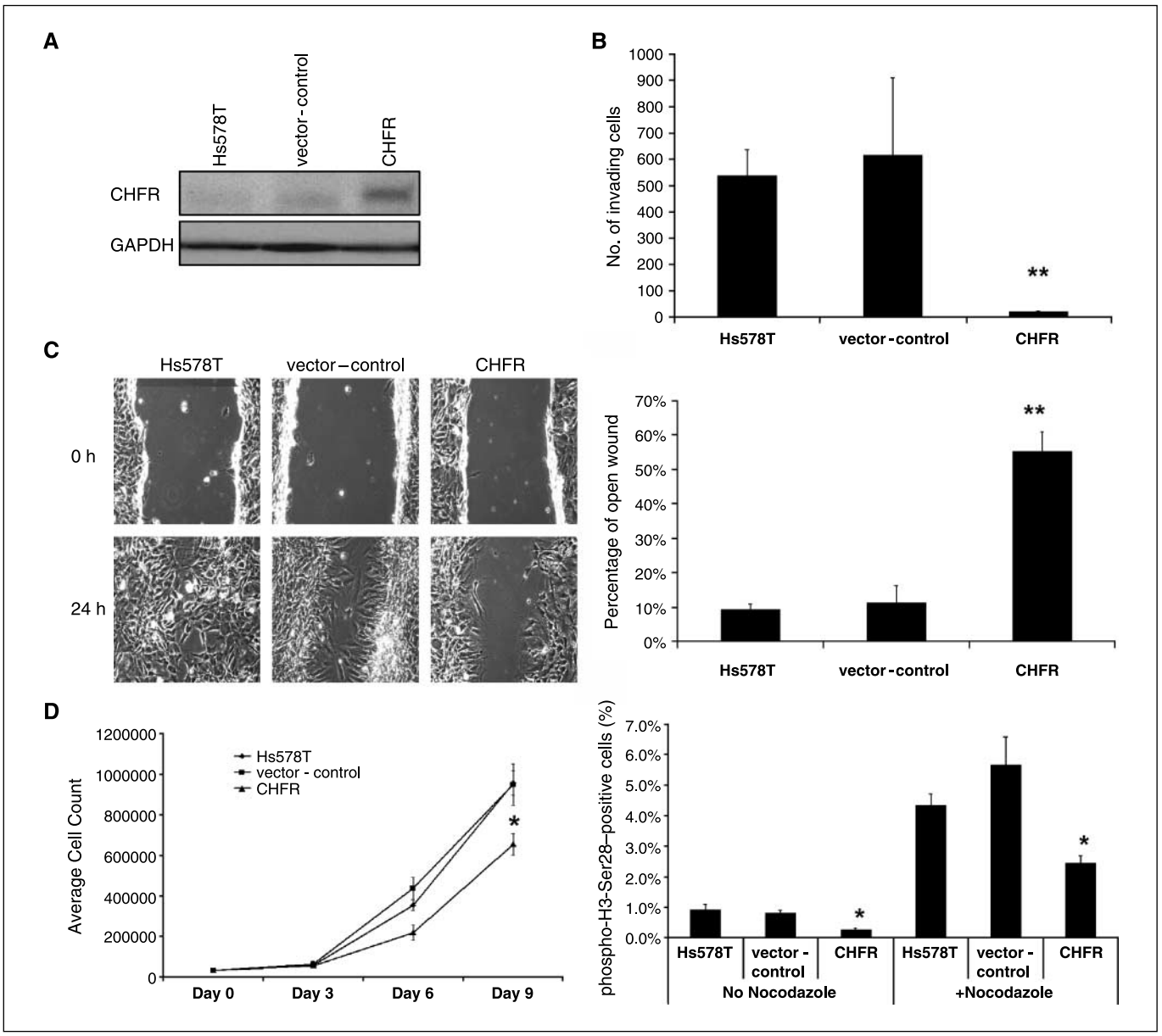

Figure 5. Stably increasing CHFR by retroviral transduction of a full-length *CHFR* cDNA construct in a BCC line, Hs578T, rescues some malignant phenotypes. *A,* Western blot showing increased CHFR expression (*top*) in cells retrovirally transduced with a Flag-tagged CHFR construct. GAPDH is used as a loading control (*bottom*). *B,* overexpression of CHFR in Hs578T cancer cells results in 25-fold loss of invasive potential through a Matrigel collagen matrix. *C, left,* phase-contrast images at ×10 magnification showing a decrease in motility for Hs578T cells following stable CHFR overexpression. *Top,* initial wound in the culture; *bottom,* wound closure after 24 h. Hs578T cells overexpressing CHFR were less motile than their control counterparts and could not sufficiently close the wound in <24 h. *Right,* graphical representation of the degree of wound closure depicted on the (*left*). Percentage of the original scraped area remaining after incubation for each cell line. *D, left,* growth curve analysis over the span of 9 d showed that Hs578T BCCs overexpressing CHFR (▲) had a slower growth rate, as indicated by a lower average cell count, than the parental (♦) or the vector negative control (■), despite being seeded at equal densities on day 0. *Right,* immunofluorescence staining for phospho–histone H3-Ser28 was used as a marker for mitotic cells. The percentage of cells positive for phospho-H3-Ser28 staining of at least 1,000 total nuclei (DAPI stained) is presented for each cell line. Overexpression of CHFR led to ~50% less mitotic cells compared with parental and empty vector controls in both untreated and nocodazole (200 ng/mL and 0.67 μmol/L) treated cells, indicating at least a partially restored checkpoint and a decrease in proliferation in untreated cells. *, $P < 0.05$; **, $P \leq 0.001$, calculated by ANOVA.

or more prominent nucleoli. In fact, changes in the number of nucleoli (more than three) are strongly correlated with a negative prognosis for survival in breast cancer patients (34). Interestingly, both IHMEC cell lines exhibited a marked increase in the number of nucleoli present in the nucleus, which was defined as three or more nucleoli, when CHFR expression was knocked down by shRNA. We found that 29% of MCF10A/CHFR shRNA cells (compared with 9% for controls; $P \leq 0.001$) and 23% of HPV4-12/CHFR shRNA cells had greater than three nucleoli (compared with 13% for controls; $P \leq 0.08$; Fig. 4*A* and *B*). This change in nucleolar organization and number may indicate alterations in cellular metabolism related to proliferation, genome organization, or gene expression.

Further evidence for the acquisition of tumorigenic phenotypes following knockdown of CHFR expression was noticed only in MCF10A cells. We observed that MCF10A cells with CHFR shRNA underwent a morphologic change following ~10 passages in

culture. These immortalized mammary epithelial cells became elongated and showed more variability in cell size, which is suggestive of the epithelial-to-mesenchymal transition that is often observed during tumorigenesis (Fig. 4*B*). Further confirmation of this transition was indicated by increased expression of vimentin, a marker of mesenchymal cells, as shown by immunofluorescence (Supplementary Fig. S1).

To determine if the loss of CHFR altered the tumorigenicity of these cell lines, parental, scrambled shRNA, and CHFR shRNA-expressing cells were suspended in a mix of soft agar and growth media and assessed for their ability to form colonies. The MCF10A cell line has already been characterized as being tumorigenic in soft agar and the loss of CHFR did not enhance this phenotype. However, the HPV4-12 cell line does not form colonies in soft agar but when CHFR expression was decreased by shRNA, there was a modest but very significant increase in the number of colonies formed in soft agar ($P < 0.001$; Fig. 4*D*), indicating that these cells potentially had become tumorigenic.

Overexpression of CHFR reverses tumorigenic phenotypes in BCCs. In the converse experiment from above, we next determined if CHFR overexpression would have any affect on a tumorigenic BCC line, Hs578T, which has no endogenous expression of CHFR protein. Hs578T cells overexpressed *CHFR* through a stably transduced retroviral construct containing the full-length cDNA (Fig. 5*A*). Ectopically expressing CHFR in these BCCs did not alter their apoptotic response to nocodazole and it did not decrease colony formation in soft agar (data not shown). However, CHFR overexpression rescued other tumorigenic phenotypes in this cell line, making the cells act less like cancer cells. Importantly, we observed a dramatic change in invasiveness and motility. When Hs578T cells had higher CHFR levels, their ability to invade through a Matrigel collagen matrix plummeted by 25-fold ($P \leq 0.001$; Fig. 5*B*). Hs578T cells overexpressing CHFR showed nearly a 6-fold decrease in motility using the scrape assay ($P \leq 0.001$; Fig. 5*C, right*). In addition, overexpression of CHFR resulted in a statistically significant decrease in growth rates ($P < 0.05$; Fig. 5*D, left*) and a decrease in mitotic cells, as indicated by positive phospho–histone H3-Ser28 staining by immunofluorescence as described above ($P < 0.05$; Fig. 5*D, right*).

Stable knockdown of CHFR expression leads to genomic instability. Because genomic instability, or aneuploidy, was reported previously for mouse embryonic fibroblasts derived from the *Chfr* knockout mouse (11), we assessed the ploidy status of IHMECs shortly after stable *CHFR* shRNA expression. Strikingly, 60% to 70% of the cells with low CHFR were aneuploid, as opposed to <5% of cells in the normally hyperdiploid (48–49 chromosomes) parental lines (Fig. 6*A* and *B*). For aneuploid cells, the number of chromosomes present ranged from 49 to >85. Aneuploidy was also confirmed by fluorescence-activated cell sorting analysis as an increase in the population of cells with greater than 4N DNA content (data not shown).

Discussion

The findings presented here contribute significantly to the characterization of *CHFR* as a tumor suppressor gene. We show that CHFR protein expression was lost in many BCC lines and primary cancers, with nearly identical percentages (41% versus 36%). In addition, we provide evidence that decreasing CHFR mRNA and protein using shRNA/siRNA resulted in two IHMEC cell lines acquiring phenotypes associated with malignant progression. These phenotypes included increased growth rates and mitotic indexes, the cells acquired the abilities of invasion and motility, and a striking percentage of cells became aneuploid. In addition, the HPV4-12 cells without CHFR were able to form colonies in soft agar, an indication of cellular transformation, and the MCF10A cells without CHFR became sensitive to microtubule poisons and underwent an epithelial-to-mesenchymal morphology change. When CHFR was overexpressed in Hs578T BCCs, the data suggested that higher CHFR levels did not have any adverse consequences in this cancer cell line and, in fact, reversed some tumorigenic phenotypes, thereby further supporting the role of CHFR as a tumor suppressor. When the CHFR expression data are combined with the results of the phenotypic analysis *in vitro* and the correlation with tumor size *in vivo*, it seems that the loss of CHFR is relevant to tumorigenesis in mammary epithelial cells.

In regards to primary invasive breast carcinoma, the correlation between CHFR staining and small tumor size, a very important prognostic indicator, is remarkable and supports a role for CHFR as a tumor suppressor. This is consistent with observations *in vitro*, in which decreased CHFR expression led to a dramatic increase in population growth rates and a higher percentage of mitotic cells. In addition, the putative association of CHFR and ER expression may provide continued support of a role for CHFR as a biomarker for breast cancer treatment. This is particularly relevant given previous clinical trials that showed ER-positive, and therefore

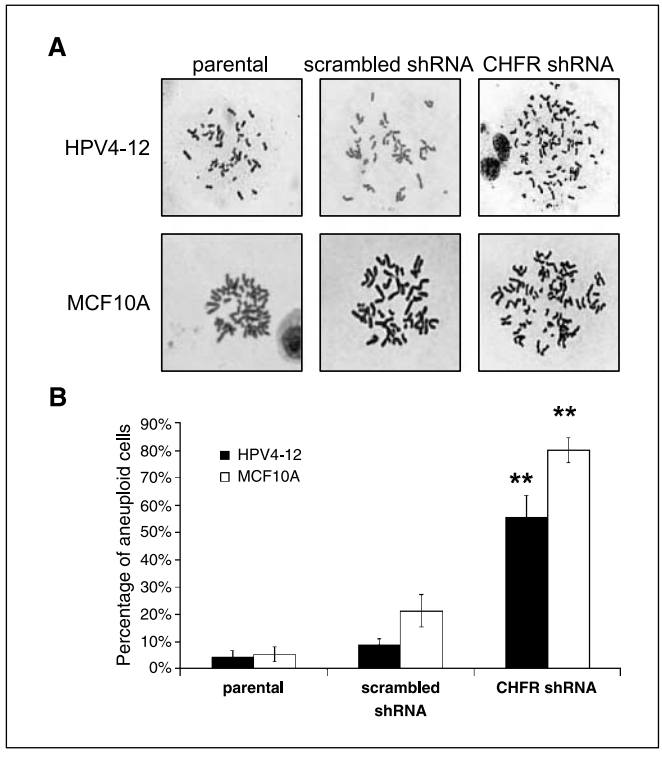

Figure 6. Decreased CHFR expression causes genomic instability. *A,* Giemsa-stained metaphase spreads of parental, negative control, and CHFR shRNA cells. IHMECs with lowered CHFR expression showed a greatly increased incidence of aneuploidy (>48 or 49 chromosomes). Both IHMEC cell lines are hyperdiploid and normally have either 48 chromosomes (MCF10A) or 49 chromosomes (HPV4-12). *B,* quantification of aneuploidy in CHFR shRNA cells showing that low CHFR expression results in 55% to 72% of the cells in the population becoming aneuploid. Percentage of aneuploid cells, from 25 counted metaphases per trial, for each cell line. **, $P \leq 0.001$, as determined by the ANOVA test for significance.

possibly CHFR-positive, breast cancers did not respond as well to paclitaxel treatment as ER-negative breast cancers (35–37). This corresponds well with previously published work describing CHFR-negative cells as sensitive to microtubule poisons in culture, undergoing apoptosis sooner than their CHFR-positive counterparts. This correlation between CHFR expression and apoptotic response to microtubule poisons was also observed in this work in the MCF10A cell line, which further substantiates a role for CHFR as a biomarker for drug response. In addition, the weak association of expression between ER and CHFR may help to elucidate another molecular pathway, in which CHFR functions to mediate cell proliferation or a common means of gene expression regulation.

Importantly, decreased CHFR expression led to an increase in the number of mitotic (metaphase and anaphase) cells in the population. Previously, this phenotype had only been described to occur in the presence of nocodazole and was thought to be due to an impaired checkpoint. However, the fact that this phenomenon also occurs without microtubule poisons suggests that CHFR can possibly play a wider role in regulating the timing of mitotic entry. This may help explain why the growth rates were faster in cells stably expressing *CHFR* shRNA and why tumors from breast cancer patients are larger when CHFR staining is absent.

Two of the most striking changes that resulted from altering CHFR expression were changes in invasion and motility of cells *in vitro*. This is the first time that CHFR has been implicated in a functional role other than cell cycle regulation. Considering its proposed role of monitoring microtubule dynamics as indicated by its initiation of the checkpoint in response to microtubule stress, it is hypothesized that CHFR has an even larger part in cytoskeletal organization, in which loss would more easily allow for the necessary reorganization of the cytoskeletal network required for motility. In addition, if the phenotypes observed in culture are found to mirror those seen in cancer patients (i.e., patients with low CHFR tumors have a higher incidence of distant metastases), then CHFR expression may be an indicator for tumor stage and/or patient prognosis.

Our report that low CHFR expression leads to genomic instability corroborates previously published work in the mouse (11). These data are suggestive of a problem with the structure or function of the mitotic spindle that is not corrected due to an impaired CHFR checkpoint. However, it could also indicate a defect in cytokinesis, which is plausible because work with the two yeast orthologues of CHFR show an interaction with the septin cytoskeletal network and they function in both the spindle checkpoint and cytokinesis (38, 39). Given the relatively frequent occurrence of low/lost CHFR in many types of tumors, this work may begin to explain the conundrum of the prevalence of aneuploidy in cancers but the lack of defective spindle checkpoint mediators, such as the MAD and BUB proteins.

It is not surprising that the same phenotypes were not always observed in the two cell lines tested. This is likely due to the unique genetic defects that caused the immortalization of the cell lines, thereby providing a clue to the genetic and physical interactions that CHFR has within the cell. Specifically, the HPV4-12 cell line was immortalized with the HPV E6/E7 protein to inhibit p53 and pRb function, whereas the MCF10A line was spontaneously immortalized following a t(3;9)(p14;p21) translocation that disrupted the *p15/p16* gene in addition to other chromosomal rearrangements (40, 41). The genetic differences may help to explain why MCF10A cells undergo a morphologic change and an increase in apoptosis in response to microtubule poisons after *CHFR* shRNA, whereas HPV4-12 cells do not. Differences may also be attributed to the fact that these two IHMEC lines are grown in different media with different levels of CO_2, but it should be noted that the media are very similar and contain nearly identical supplements.

This work on the phenotypic changes that arise *in vitro* with CHFR expression variation provides a unique insight as to what may happen in cancer patients and presents many new avenues through which to study CHFR expression, function, and molecular interactions. We report for the first time a correlation between CHFR levels and clinicopathologic variables in primary breast cancer, tumor size and perhaps ER status. We also comprehensively characterize the phenotypic changes that resemble cellular transformation in normal IHMEC cells when CHFR expression is substantially reduced. Through the combined findings of this work, we find the loss of CHFR to be an interesting dichotomy in breast cancer. This report shows that, on one hand, the loss of CHFR expression may indicate a larger and more aggressive tumor, whereas, in a surprising beneficial twist, it also makes the cancer cells sensitive to traditional chemotherapeutic agents that target the microtubules. It seems that as evidence builds, CHFR is gaining more time in the spotlight as a novel tumor suppressor as it aspires to be the next biomarker in cancer characterization.

Acknowledgments

Received 11/7/2006; revised 3/4/2007; accepted 4/5/2007.

Grant support: Department of Defense Breast Cancer Research Predoctoral Fellowship #BC050310 and NIH National Research Service Award #5-T32-GM07544 from the National Institute of General Medicine Sciences (L.M. Privette); NIH National Cancer Institute (NCI) grant RO1CA072877 (E.M. Petty); and NIH NCI grants K08CA090876 and R01CA107469 and Department of Defense grant DAMD17-01-1-490 (C.G. Kleer).

The costs of publication of this article were defrayed in part by the payment of page charges. This article must therefore be hereby marked *advertisement* in accordance with 18 U.S.C. Section 1734 solely to indicate this fact.

We thank Esther Peterson for helpful suggestions and discussion; Nancy McAnsh and Donita Sanders for technical assistance with immunohistochemistry protocols; Thomas Giordano, M.D., for primary normal breast tissue samples; and Stephen Ethier, Ph.D., for the HPV and SUM breast cell lines.

References

1. Scolnick DM, Halazonetis TD. Chfr defines a mitotic stress checkpoint that delays entry into metaphase. Nature 2000;406:430–5.
2. Summers MK, Bothos J, Halazonetis TD. The CHFR mitotic checkpoint protein delays cell cycle progression by excluding cyclin B1 from the nucleus. Oncogene 2005; 24:2589–98.
3. Dang C, Hudis C. Adjuvant taxanes in the treatment of breast cancer: no longer at the tip of the iceberg. Clin Breast Cancer 2006;7:51–8.
4. Sakai M, Hibi K, Kanazumi N, et al. Aberrant methylation of the CHFR gene in advanced hepatocellular carcinoma. Hepatogastroenterology 2005;52:1854–7.
5. Satoh A, Toyota M, Itoh F, et al. Epigenetic inactivation of CHFR and sensitivity to microtubule inhibitors in gastric cancer. Cancer Res 2003;63:8606–13.
6. Chaturvedi P, Sudakin V, Bobiak ML, et al. Chfr regulates a mitotic stress pathway through its RING-finger domain with ubiquitin ligase activity. Cancer Res 2002;62:1797–801.
7. Ogi K, Toyota M, Mita H, et al. Small interfering RNA-induced CHFR silencing sensitizes oral squamous cell cancer cells to microtubule inhibitors. Cancer Biol Ther 2005;4:773–80.
8. Kang D, Chen J, Wong J, Fang G. The checkpoint protein Chfr is a ligase that ubiquitinates Plk1 and inhibits Cdc2 at the G_2 to M transition. J Cell Biol 2002;156:249–59.
9. Matsusaka T, Pines J. Chfr acts with the p38 stress kinases to block entry to mitosis in mammalian cells. J Cell Biol 2004;166:507–16.
10. Shtivelman E. Promotion of mitosis by activated protein kinase B after DNA damage involves polo-like kinase 1 and checkpoint protein CHFR. Mol Cancer Res 2003;1:959–69.
11. Yu X, Minter-Dykhouse K, Malureanu L, et al. Chfr is required for tumor suppression and Aurora A regulation. Nat Genet 2005;37:401–6.

12. Brandes JC, van Engeland M, Wouters KA, Weijenberg MP, Herman JG. CHFR promoter hypermethylation in colon cancer correlates with the microsatellite instability phenotype. Carcinogenesis 2005;26:1152–6.
13. Cheung HW, Ching YP, Nicholls JM, et al. Epigenetic inactivation of CHFR in nasopharyngeal carcinoma through promoter methylation. Mol Carcinog 2005;43:237–45.
14. Corn PG, Summers MK, Fogt F, et al. Frequent hypermethylation of the 5′ CpG island of the mitotic stress checkpoint gene Chfr in colorectal and non-small cell lung cancer. Carcinogenesis 2003;24:47–51.
15. Honda T, Tamura G, Waki T, Kawata S, Nishizuka S, Motoyama T. Promoter hypermethylation of the Chfr gene in neoplastic and non-neoplastic gastric epithelia. Br J Cancer 2004;90:2013–6.
16. Mariatos G, Bothos J, Zacharatos P, et al. Inactivating mutations targeting the chfr mitotic checkpoint gene in human lung cancer. Cancer Res 2003;63:7185–9.
17. Mizuno K, Osada H, Konishi H, et al. Aberrant hypermethylation of the CHFR prophase checkpoint gene in human lung cancers. Oncogene 2002;21:2328–33.
18. Shibata Y, Haruki N, Kuwabara Y, et al. Chfr expression is downregulated by CpG island hypermethylation in esophageal cancer. Carcinogenesis 2002;23:1695–9.
19. Tokunaga E, Oki E, Nishida K, et al. Aberrant hypermethylation of the promoter region of the CHFR gene is rare in primary breast cancer. Breast Cancer Res Treat 2006;97:199–203.
20. Toyota M, Sasaki Y, Satoh A, et al. Epigenetic inactivation of CHFR in human tumors. Proc Natl Acad Sci U S A 2003;100:7818–23.
21. Andrieux J, Demory JL, Morel P, et al. Frequency of structural abnormalities of the long arm of chromosome 12 in myelofibrosis with myeloid metaplasia. Cancer Genet Cytogenet 2002;137:68–71.
22. Aubele M, Auer G, Braselmann H, et al. Chromosomal imbalances are associated with metastasis-free survival in breast cancer patients. Anal Cell Pathol 2002;24:77–87.
23. Dohna M, Reincke M, Mincheva A, Allolio B, Solinas-Toldo S, Lichter P. Adrenocortical carcinoma is characterized by a high frequency of chromosomal gains and high-level amplifications. Genes Chromosomes Cancer 2000;28:145–52.
24. Heidenblad M, Schoenmakers EF, Jonson T, et al. Genome-wide array-based comparative genomic hybridization reveals multiple amplification targets and novel homozygous deletions in pancreatic carcinoma cell lines. Cancer Res 2004;64:3052–9.
25. Rutherford S, Hampton GM, Frierson HF, Moskaluk CA. Mapping of candidate tumor suppressor genes on chromosome 12 in adenoid cystic carcinoma. Lab Invest 2005;85:1076–85.
26. Ethier SP, Mahacek ML, Gullick WJ, Frank TS, Weber BL. Differential isolation of normal luminal mammary epithelial cells and breast cancer cells from primary and metastatic sites using selective media. Cancer Res 1993;53:627–35.
27. Neve RM, Chin K, Fridlyand J, et al. A collection of breast cancer cell lines for the study of functionally distinct cancer subtypes. Cancer Cell 2006;10:515–27.
28. Erson AE, Niell BL, DeMers SK, Rouillard JM, Hanash SM, Petty EM. Overexpressed genes/ESTs and characterization of distinct amplicons on 17q23 in breast cancer cells. Neoplasia 2001;3:521–6.
29. Van den Eynden GG, Van der Auwera I, Van Laere S, et al. Validation of a tissue microarray to study differential protein expression in inflammatory and non-inflammatory breast cancer. Breast Cancer Res Treat 2004;85:13–22.
30. Kleer CG, Cao Q, Varambally S, et al. EZH2 is a marker of aggressive breast cancer and promotes neoplastic transformation of breast epithelial cells. Proc Natl Acad Sci U S A 2003;100:11606–11.
31. Erson AE, Petty EM. CHFR-associated early G_2/M checkpoint defects in breast cancer cells. Mol Carcinog 2004;39:26–33.
32. Goto H, Tomono Y, Ajiro K, et al. Identification of a novel phosphorylation site on histone H3 coupled with mitotic chromosome condensation. J Biol Chem 1999;274:25543–9.
33. Vermes I, Haanen C, Steffens-Nakken H, Reutelingsperger C. A novel assay for apoptosis. Flow cytometric detection of phosphatidylserine expression on early apoptotic cells using fluorescein labelled Annexin V. J Immunol Methods 1995;184:39–51.
34. van Diest PJ, Mouriquand J, Schipper NW, Baak JP. Prognostic value of nucleolar morphometric variables in cytological breast cancer specimens. J Clin Pathol 1990;43:157–9.
35. Berry DA, Cirrincione C, Henderson IC, et al. Estrogen-receptor status and outcomes of modern chemotherapy for patients with node-positive breast cancer. JAMA 2006;295:1658–67.
36. Poole C. Adjuvant chemotherapy for early-stage breast cancer: the tAnGo trial. Oncology (Huntingt) 2004;18:23–6.
37. Sezgin C, Karabulut B, Uslu R, et al. Potential predictive factors for response to weekly paclitaxel treatment in patients with metastatic breast cancer. J Chemother 2005;17:96–103.
38. Fraschini R, Bilotta D, Lucchini G, Piatti S. Functional characterization of Dma1 and Dma2, the budding yeast homologues of *Schizosaccharomyces pombe* Dma1 and human Chfr. Mol Biol Cell 2004;15:3796–810.
39. Guertin DA, Venkatram S, Gould KL, McCollum D. Dma1 prevents mitotic exit and cytokinesis by inhibiting the septation initiation network (SIN). Dev Cell 2002;3:779–90.
40. Band V, Zajchowski D, Kulesa V, Sager R. Human papilloma virus DNAs immortalize normal human mammary epithelial cells and reduce their growth factor requirements. Proc Natl Acad Sci U S A 1990;87:463–7.
41. Cowell JK, LaDuca J, Rossi MR, Burkhardt T, Nowak NJ, Matsui S. Molecular characterization of the t(3;9) associated with immortalization in the MCF10A cell line. Cancer Genet Cytogenet 2005;163:23–9.